

FEEDFORWARD BANG-BANG CONTROL DESIGN FOR ELECTRO-PNEUMATIC PROTECTION VALVES

Huba NÉMETH*, László PALKOVICS* and Katalin M. HANGOS**

*Knorr-Bremse Research & Development Centre
H-1119, Budapest, Major u. 69., Hungary.

**Systems and Control Laboratory
Computer and Automation Research Institute
Hungarian Academy of Sciences
H-1518, Budapest, P.O.B. 63., Hungary

Received: Oct. 17, 2003

Abstract

A direct method of nonlinear control design is presented in this paper that is based on a simplified hybrid model of the electro-pneumatic protection valve used for circuit pressure limiting function of commercial vehicle air supply systems. The dynamic model analysis is performed to meet the control design requirements, the hybrid behaviour is investigated in more details. The proposed bang-bang controller fulfils the predefined optimality criteria that is achieved by numeric optimization.

Keywords: bang-bang control, brakes, convex optimization, feedforward control, nonlinear models, pneumatic systems

1. Introduction

Lately, the progression of electrical systems has been highly developed in the automotive sector. It has pushed many functions not realized before due to complexity. On the other hand cost reduction is another main driver.

Protection valves have been common parts in the brake systems of commercial vehicles for a long time. However, their function was always limited to their original aim. With the introduction of electro-magnetic actuators to improve their original function, additional tasks are also possible to be implemented. A new function is the limiting of the circuit pressure according to dynamic set-point demands. This enables the omission of conventional pressure limiting valves.

This paper focuses on the model analysis and design of a controller that is able to fulfil circuit pressure limiting using an electro-pneumatic protection valve.

Recently an exhaustive modelling was performed on the single circuit protection valve [6]. This model was originally developed from first engineering principles in the form of a lumped hybrid index-1 model. This model was recognized to be too complex for control design purposes. Therefore, model simplification was performed to reduce the dimension of the state- and parameter vector and the complexity of the equations [9]. The simplification used L_2 norms to evaluate the error caused by the simplifying assumptions, which were made using engineering

insight and operation experience on the behavior of the real system. The resulted simplified model preserved the engineering meaning of its variables and parameters, while the number of the state variables and parameters was reduced significantly.

The obtained simplified model was the object of model calibration and validation [8]. The validated model fulfilled the predefined modelling error tolerances and serves as basis for model analysis and control design.

The control of electro-pneumatic valves is usually performed using PID or fuzzy techniques [10, 12], at the same time nonlinear model based, especially hybrid control is even more spreading in the automotive sector [3]. Despite of the above mentioned papers, the control of electro-pneumatic protection valves has not yet matured and it is still an open research area. This paper presents an attempt of solving this problem by optimal control techniques.

The objective of optimal control is to minimize predefined performance criteria. A well known example is the LQR control in case of FDLTI systems, where an exact analytical solution exists. The advantageous properties (gain margin, phase margin) of this feedback are also widely known [4]. In case of nonlinear systems, however, this analytic solution does not exist in general. So one is usually faced to numeric optimization techniques to reach a certain optimality [11].

The Outline of the paper is as follows: In the first part the basic notions, the nonlinear model of the electro-pneumatic protection valve and its hybrid behavior are briefly described. The second part contains the analysis of the model properties and design of the output feedforward bang-bang controller. Finally, conclusions are drawn.

The detailed model analysis and control design presented in this paper can be found in a technical report [7].

2. The State Space Model

2.1. System Description

The single circuit protection valve unit consists of the following elements (see Fig. 1):

- *Input chamber* (1) This chamber has two output flows towards the protection valve and the magnet valve.
- *Output chamber* (2) This chamber has an input air flow from the protection valve and an output towards the brake system or other consumers.
- *Control chamber* (3) This chamber has a single port that can be connected either to the input chamber or the ambient by the magnet valve.
- *Input piping* (4) It connects the input chamber to the protection valve.
- *Output piping* (5) This connects the protection valve to the output chamber.
- *Protection valve* (6) The valve has an input connection from the input chamber through the input pipe and an output to the output chamber through the output pipe.

- *Control magnet valve (7)* It is a 3/2-way valve with solenoid excitation with one input port connected to the input chamber and two output ports. The one is going to the control chamber and the other one is exhausting to the environment.

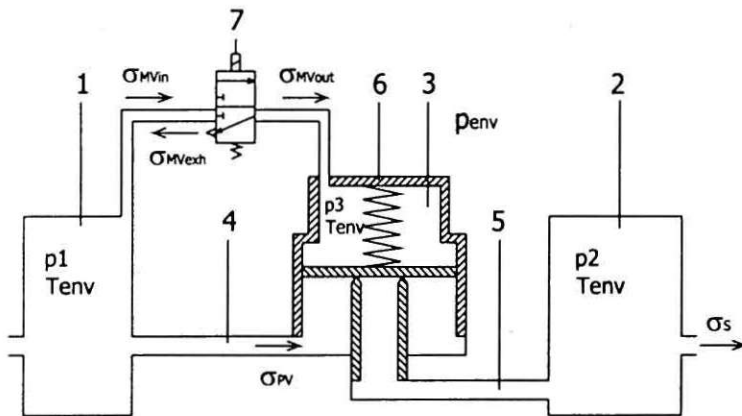


Fig. 1. Scheme of the single electro-pneumatic protection valve unit with the important variables

2.2. Model Equations

According to the results of the model simplification [9] the model variables are formed as follows.

State Vector The state vector includes the pressures of the output- and control chambers, speed and position of the two moving elements and the solenoid current:

$$\mathbf{x} = [p_2 \quad p_3 \quad x_{PV} \quad v_{PV} \quad x_{MV} \quad v_{MV} \quad I_{MV}]^T.$$

Disturbance Vector The disturbance vector has the input chamber pressure, circuit air consumption as key disturbances and the environment temperature as slowly changing disturbance:

$$\mathbf{d} = [p_1 \quad \sigma_s \quad T_{env}]^T.$$

Input Vector The input vector includes one member only, which is the excitation voltage of the magnet valve:

$$\mathbf{u} = [U].$$

Measured Output The measurable state variables and disturbances are formed as measured output including the three pressures, the solenoid current and circuit air consumption presence as discrete variable:

$$\mathbf{y} = [p_2 \quad p_3 \quad I_{MV} \quad p_1 \quad \lambda_S]^T.$$

Performance Output The performance output is the output chamber pressure:

$$\mathbf{z} = [p_2].$$

2.2.1. State Equation

The simplified state space model is in the following form:

$$\begin{bmatrix} \dot{p}_2 \\ \dot{p}_3 \\ \dot{x}_{PV} \\ \dot{v}_{PV} \\ \dot{x}_{MV} \\ \dot{v}_{MV} \\ \dot{I}_{MV} \end{bmatrix} = \begin{bmatrix} f_1(\mathbf{x}, \mathbf{d}) \\ f_2(\mathbf{x}, \mathbf{d}) \\ f_3(\mathbf{x}, \mathbf{d}) \\ f_4(\mathbf{x}, \mathbf{d}) \\ f_5(\mathbf{x}, \mathbf{d}) \\ f_6(\mathbf{x}, \mathbf{d}) \\ f_7(\mathbf{x}, \mathbf{d}) \end{bmatrix} + \begin{bmatrix} 0 \\ 0 \\ 0 \\ 0 \\ 0 \\ 0 \\ \frac{(R_{ML} + \frac{x_{MV}}{\mu_0 A_{MB}})}{N^2} \end{bmatrix} \mathbf{u}, \quad (1)$$

where the nonlinear state functions with all constitutive relations substituted are as:

$$f_1 = \frac{RT_{env}}{V_2} \left(\frac{\alpha_{PV} d_2 \pi x_{PVmax} p_1 \xi(p_1, p_2)}{1 + e^{-u_{PV}(x_{PV} - x_{PVmax}/2)}} - \sigma_S \right), \quad (2)$$

$$f_2 = \frac{RT_{env}}{V_3} \left(\frac{\alpha_{MV} d_{MVin}^2 \pi p_1 \xi(p_1, p_3)}{4 + 4e^{-u_{MV}(x_{MVmax}/2 - x_{MV})}} - \frac{\alpha_{MV} d_{MVexh}^2 \pi p_3 \xi}{4 + 4e^{-u_{MV}(x_{MV} - x_{MVmax}/2)}} \right), \quad (3)$$

$$f_3 = v_{PV}, \quad (4)$$

$$f_4 = \frac{p_1 (d_1^2 - d_2^2) \frac{\pi}{4} + p_2 d_2^2 \frac{\pi}{4} - p_3 d_1^2 \frac{\pi}{4} - c_{PV}(x_{PV} + x_{0PV}) - k_{PV} v_{PV}}{m_{PV}}, \quad (5)$$

$$f_5 = v_{MV}, \quad (6)$$

$$f_6 = \frac{N^2 I_{MV}^2}{2m_{MV} (R_{ML} + \frac{x_{MV}}{\mu_0 A_{MB}})^2 \mu_0 A_{MB}} - \frac{c_{MV}(x_{MV} + x_{0MV}) + k_{MV} v_{MV}}{m_{MV}}, \quad (7)$$

$$f_7 = \frac{I_{MV} v_{MV}}{(R_{ML} + \frac{x_{MV}}{\mu_0 A_{MB}}) \mu_0 A_{MB}} - \frac{R I_{MV} (R_{ML} + \frac{x_{MV}}{\mu_0 A_{MB}})}{N^2}, \quad (8)$$

where

$$\xi(p_1, p_2) = \sqrt{\frac{2\kappa \left(\left(\frac{p_2}{p_1} \right)^{\frac{2}{\kappa}} - \left(\frac{p_2}{p_1} \right)^{\frac{\kappa+1}{\kappa}} \right)}{(\kappa - 1)RT_{env}}},$$

$$\xi(p_1, p_3) = \sqrt{\frac{2\kappa \left(\left(\frac{p_3}{p_1} \right)^{\frac{2}{\kappa}} - \left(\frac{p_3}{p_1} \right)^{\frac{\kappa+1}{\kappa}} \right)}{(\kappa - 1)RT_{env}}},$$

$$\zeta = \sqrt{\frac{2\kappa \left(\left(\frac{2}{\kappa+1} \right)^{\frac{2}{\kappa-1}} - \left(\frac{2}{\kappa+1} \right)^{\frac{\kappa+1}{\kappa-1}} \right)}{(\kappa - 1)RT_{env}}}.$$

2.2.2. Output Equation

The measured output is written as the following state-affine equation:

$$\mathbf{y} = \begin{bmatrix} 1 & 0 & 0 & 0 & 0 & 0 & 0 & 0 \\ 0 & 1 & 0 & 0 & 0 & 0 & 0 & 0 \\ 0 & 0 & 0 & 0 & 0 & 0 & 0 & 1 \\ 0 & 0 & 0 & 0 & 0 & 0 & 0 & 0 \\ 0 & 0 & 0 & 0 & 0 & 0 & 0 & 0 \end{bmatrix} \mathbf{x} + \begin{bmatrix} 0 \\ 0 \\ 0 \\ p_1 \\ \text{sgn}(\sigma_5) \end{bmatrix}. \quad (9)$$

The performance output is generated from the measured output by the following simple equation:

$$\mathbf{z} = [1 \ 0 \ 0 \ 0 \ 0] \mathbf{y}. \quad (10)$$

2.3. Hybrid Behavior

The system contains several parts that exhibit discrete behavior. This means, that the equations, which describe the dynamic behavior of the corresponding subsystem vary according to certain circumstances [1] (discrete-continuous model definition).

This implies that the above described equations refer to a dedicated hybrid state only. Some parts may change in different domains of the state space.

The simplified model contains three subsystems comprising hybrid properties: (i) protection valve piston and (ii) magnet valve armature due to stroke limitation having three hybrid states each and finally the (iii) protection valve/magnet valve air flow part due to sonic/subsonic streaming features including six hybrid states.

2.4. Operation Domain

By experimental investigations of the system the following operation domain can be realized. The state vector members are restricted as follows:

$$\begin{aligned} 10^5 \leq p_2 \leq 1.3 \cdot 10^6 \text{ [Pa]}, & \quad 10^5 \leq p_3 \leq 1.3 \cdot 10^6 \text{ [Pa]}, & \quad 0 \leq x_{pV} \leq 0.002 \text{ [m]}, \\ -1 \leq v_{pV} \leq 1 \text{ [m/s]}, & \quad 0 \leq x_{MV} \leq 0.0005 \text{ [m]}, & \quad -1 \leq v_{MV} \leq 1 \text{ [m/s]}, \\ 0 \leq I_{MV} \leq 1 \text{ [A]}. & & \end{aligned}$$

The input variable has the following limits:

$$0 \leq U \leq 24 \text{ [V]}.$$

The disturbance variables are limited to the following range:

$$10^5 \leq p_1 \leq 1.3 \cdot 10^6 \text{ [Pa]}, \quad 0 \leq \sigma_S \leq 0.05 \text{ [kg/s]}, \quad 288 \leq T_{\text{env}} \leq 303 \text{ [K]}.$$

3. Model Analysis

3.1. Nonlinear Input-affine State Equation

The nonlinear state equation transformed into intensive variable form described in Eqs. (1)–(8) can be expressed in a canonical form called input-affine state equation [2] as:

$$\frac{d\mathbf{x}}{dt} = f(\mathbf{x}, \mathbf{d}) + g(\mathbf{x})\mathbf{u}. \quad (11)$$

Observe that the $g(\mathbf{x})$ depends linearly on the state vector, i.e. the effect of the input is bilinear to the time derivative of the state vector. Moreover, only one state variable is affected directly by the input.

3.2. Hybrid Analysis

The above state space model is a set of ordinary differential equations (ODEs), where all the state functions are explicitly defined in all of the hybrid states (i.e. there are no algebraic constraints on the state variables). Moreover, all the hybrid states define smooth state functions on the boundary of the corresponding hybrid domain. This means, that the derivatives of the state variables are piecewise defined continuous functions as the system transits from one hybrid state to another, i.e. *the state variables are smooth functions in at least first order.*

3.2.1. Hybrid State Transitions

The state transitions of a hybrid part define which are the possible transitions, that can occur by the inputs of the system if the system is in the corresponding hybrid state.

The first two hybrid parts have three hybrid states each where a sequential state transition can occur driven by the manipulable input. The state transition diagram of the protection valve piston with stroke limitation can be seen in Fig. 2. The state transition graph of the magnet valve stroke limitation is exactly the same with hybrid state 1 and 3 defining the limited positions, and 2 refers to the intermediate position.

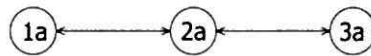


Fig. 2. The hybrid state transition graph of the protection valve stroke limiting

The third hybrid part that defines the state equations of the chamber pressures varies depending on the input considered there. If all the system inputs (manipulable and non-manipulable, i.e. disturbances) are considered, then all the hybrid states can be reached from any other one. If the manipulable input is considered only, then only four hybrid states are triggered. The state transition diagram of this subsystem can be seen in Fig. 3.

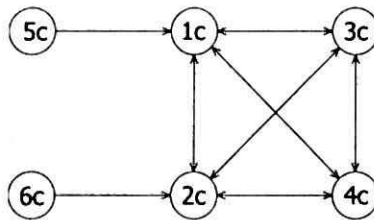


Fig. 3. The hybrid state transition graph of the air flow hybrid part considering manipulable input only

3.2.2. State Reachable Property

A hybrid system is called (hybrid state) controllable or reachable if one can always find an appropriate input function to move the system from its given initial hybrid state to a specified final state in finite time [1]. This applies to every final state pairs

given initial state. This means, when the state transition graph as a directed graph is in itself a strongly connected component then the underlying system is reachable. Note that a directed graph is a strongly connected component in itself if there is at least one directed path from any vertex to any other vertex.

In conclusion, the first two hybrid parts show (hybrid state) reachable property because the appropriate input function can always be found that moves the system from one hybrid state to the other one moreover no deadlocks are found.

The state transition graph of the third hybrid part shows that states 5c and 6c are not triggered directly by the manipulable input, just the rest of the hybrid states (1c–4c), which form strongly connected components in themselves. However, this does not cause a problem for a controller because the target operation domain is entirely covered by the triggered hybrid states (1c–4c). Deadlocks are not found in this hybrid part, too.

3.3. Structural Properties

Structural properties are held for a class of system with the same structure. The structure of a general matrix \mathbf{W} is given by the structure matrix $[\mathbf{W}]$ whose entries are defined as follows [1]:

$$[w]_{ij} = \begin{cases} 0 & \text{if } w_{ij} = 0, \\ * & \text{otherwise,} \end{cases} \quad (12)$$

where $*$ is a non-zero undetermined entry.

The dimension of structure matrices, analogous to the LTI system matrices, are defined by the structure indices n , r and m as follows:

$$[\mathbf{A}] \in \mathbb{R}^{n \times n}, [\mathbf{B}] \in \mathbb{R}^{n \times r}, [\mathbf{C}] \in \mathbb{R}^{m \times n}. \quad (13)$$

The structure matrices of the single electro-pneumatic protection valve model are given as follows:

$$[\mathbf{A}] = \begin{bmatrix} 0/* & 0 & * & 0 & 0 & 0 & 0 \\ 0 & * & 0 & 0 & * & 0 & 0 \\ 0 & 0 & 0 & * & 0 & 0 & 0 \\ * & * & * & * & 0 & 0 & 0 \\ 0 & 0 & 0 & 0 & 0 & * & 0 \\ 0 & 0 & 0 & 0 & * & * & * \\ 0 & 0 & 0 & 0 & * & * & * \end{bmatrix},$$

$$\begin{aligned}
 [\mathbf{B}] &= \begin{bmatrix} 0 \\ 0 \\ 0 \\ 0 \\ 0 \\ 0 \\ * \end{bmatrix}, \\
 [\mathbf{C}] &= \begin{bmatrix} * & 0 & 0 & 0 & 0 & 0 & 0 \\ 0 & * & 0 & 0 & 0 & 0 & 0 \\ 0 & 0 & 0 & 0 & 0 & 0 & * \\ 0 & 0 & 0 & 0 & 0 & 0 & 0 \\ 0 & 0 & 0 & 0 & 0 & 0 & 0 \end{bmatrix}.
 \end{aligned} \tag{14}$$

Note that the first entry of the state structure matrix changes depending on the hybrid state the system is working in (it is 0 in 2c, 4c and 6c hybrid states otherwise *). All other structure matrix entries are hybrid state-invariant.

The first important property of the state structure matrix is the presence of full structural rank regardless the value of the altering entry.

Using the block matrix $[\mathbf{A} \ \mathbf{B}]$ one can conclude that the system is *structurally (state) controllable* due to the full rank with the exception of null measure sets [1]. This is a hybrid state-invariant property of the system.

Similarly the rank of block matrix $[\mathbf{C} \ \mathbf{A}]^T$ gives that the investigated system is *structurally (state) observable* as of having full rank with the same exception of null measure sets [1]. This feature is also not depending on the altering entry of the state structure matrix.

The structure graph based on the structure matrices is depicted in Fig. 4, where the double circle denotes the input variable, triangles are the disturbance entries, single circles are the state variable terms and rectangles are used for output entries.

Using the state structure matrix and structure graph of the system, the relative degree of the system can also be determined [1]. The relative degree is exactly equal to the number of times one has to differentiate the output $\mathbf{y}(t)$ in order that the input $\mathbf{u}(t)$ appears in the equation. This is equal to the length of the minimal path between the vertices that represent $\mathbf{u}(t)$ and $\mathbf{y}(t)$. This way one can conclude that the investigated system is of *maximum relative degree* with respect to the performance output (p_2) that is hybrid state-invariant.

3.4. Stability Analysis

The global asymptotic stability of the system can be proven by finding a Lyapunov-function, which is a dissipative scalar positive definite function. Quadratic Lyapunov function candidates can be used for the system to determine the domain of its asymptotic stability [2].

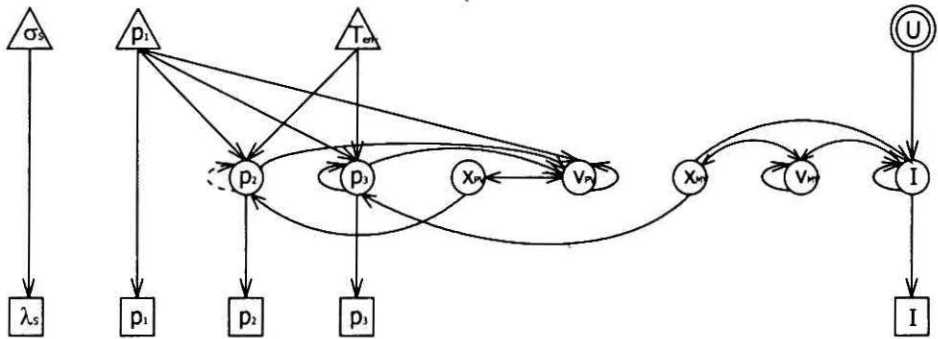


Fig. 4. The structure graph of the model

The investigated system shows *locally asymptotically stable* (open loop stable) behavior near to a steady-state operating point when its state variables are tending to the same values from any initial state considering constant input and disturbance variables. An important steady-state value of the system with respect to the pressure limiting control problem is when the initial conditions imply the opening state of the protection valve piston and zero input voltage is applied:

$$\mathbf{x}_\infty = [p_1 \quad p_{env} \quad x_{PVmax} \quad 0 \quad x_{MVmax} \quad 0 \quad 0]^T.$$

Experimental step response tests show that the valve system exhibits the locally asymptotically stable behavior in a wide neighbourhood of this steady-state value.

4. Feedforward Bang-Bang Control Design

4.1. Control Aims

The following control aims are considered for the circuit pressure limiting function of the electro-pneumatic protection valve:

- C1. The circuit pressure has to be limited according to a static set point pressure with $5 \cdot 10^4$ Pa tolerance.
- C2. The pressure breakdown caused by the external air consumption in the circuit should be minimized.
- C3. The control has to be robust with respect to the parameters of the simplified model.

4.2. Control Constraint: Two-level Input

There is an important constraint applied to the system input that influences the type of the controller. The input voltage can take two levels only. This is imposed by the simple electronic actuator (transistor) connected to the solenoid valve, which can switch on or off the supply voltage to the solenoid. The level of input voltage in switch on phase is determined by the supply voltage, in off phase it is switched to the ground.

The above constraint implies that the controller should be a member of the bang-bang controller family, where the manipulable variable is the actuation time.

4.3. Disturbance Observation

Having investigated the sensitivity of the model by the disturbance vector members the result shows that the model is sensitive to the air consumption (σ_S) and input pressure (p_1) disturbance signals. The last term (T_{env}) does not produce a significant effect on the output variables, moreover its operation range is small and the change of this disturbance signal is definitely slow (some K per hour) compared to the processes in the protection valve.

Based on these results one can conclude that the first two disturbance terms (σ_S , p_1) are key information for the pressure limiter controller as having high effect and considerable dynamic behavior.

Since only one (p_1) of the key disturbances is directly measurable, while the other is known in terms of an indicator discrete signal only (λ_S – practically the presence of the consumption), the σ_S signal needs to be estimated from the measurable signals using an observer.

The high relative degree of the system and the a priori unknown duration of the air consumption imply that the pressure limiting control problem for avoiding overshoots is not causal with respect to the air consumption disturbance signal. Therefore a restricted version of the problem is investigated further.

Besides of restricting the problem to a causal one by simplifying assumptions, these assumptions below ensure the above mentioned observer structure simple:

- A1. The air consumption caused by the brake system is constant over time during a single brake intervention.
- A2. The duration of the air consumption is constant.

In this restricted case the observation can be based on the initial part of a brake intervention when the air consumption is already present ($\lambda_S = 1$) but the protection valve piston is still closed. The closed piston state is obtained from Eq.5, meanwhile the pressure derivative of the output chamber is only affected by the external air consumption in Eq.2, because the first term between the brackets is zero under closed piston position.

4.4. Control Principle

As the control problem is basically the rejection of the disturbance made by external air consumption, a *fixed programme feedforward control* was considered. The control design consists of two steps.

- (i) The input profile applied to the system is obtained by off line step response optimizations that consider the control aims and the input constraint assuming fixed levels of the major disturbances. From the results a fixed input programme table is constructed.
- (ii) The signals of the measured output are then used to determine the actual input programme to fulfil the control aims.

The fixed programme table is divided into 11 parts according to the values of the considered two disturbance signals (σ_s , p_1). The air consumption signal range is equally divided into 4 parts along the operation domain of the signal, while the input pressure signal range is also divided into 4 parts but unequally, the pressure range below the set point plus overshoot tolerance $((9.5 + 0.5) \cdot 10^5 \text{ Pa})$ forms one part (P1 programme). Above this pressure level three equally divided parts are made. The programme table layout is shown in *Table 1*.

Table 1. Layout of the Fixed Programme Table

		p_1 [Pa]			
		$< 10^6$	10^6	$1.15 \cdot 10^6$	$1.3 \cdot 10^6$
	0		P2		
σ_s	0.016	P1	P3	P4	P5
[kg/s]	0.033		P6	P7	P8
	0.05		P9	P10	P11

P1 programme includes full magnet valve release (opened protection valve during air consumption presence), P2 programme has full magnet valve excitation (closed protection valve during air consumption presence). The other programmes include individual input voltage profiles obtained from the off line optimization.

The appropriate fixed programme is selected based on the air consumption estimated by the observer and on the measured input pressure. The nearest lower air consumption is selected, while the nearest upper input pressure gives the actual fixed programme. These considerations are made to avoid the overshoot rather than the undershoot. The scheme of the closed loop system is depicted in *Fig. 5*.

4.5. The Optimization Problem

This section describes how an element program P_i in the fixed programme table is determined by off-line optimization.

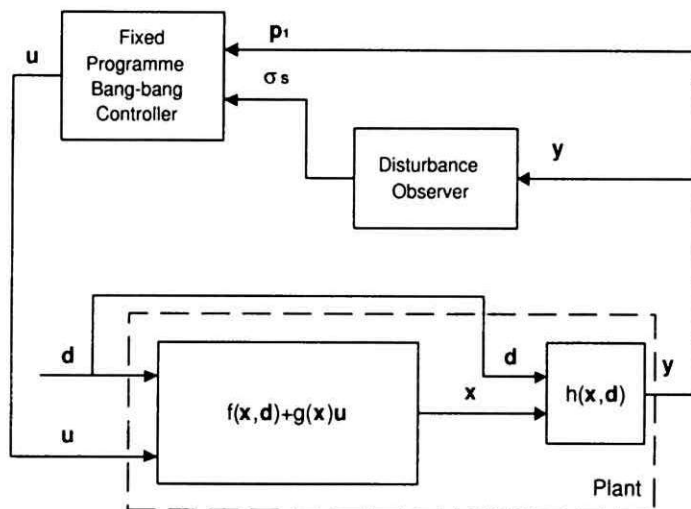


Fig. 5. Block scheme of the closed loop system

4.5.1. Optimization Method

The control design target can be mathematically formulated according to the pre-defined control aims as the following cost functional to be minimized:

$$J(\mathbf{z}, \mathbf{u}) = \int_0^{\infty} \left(Q(\Delta \mathbf{z}) \Delta \mathbf{z}^2 + S \left(\frac{d\mathbf{u}}{dt} \right)^2 \right) dt \quad (15)$$

where $\Delta \mathbf{z} = \mathbf{z} - \mathbf{z}_{set}$ is the performance output set point deviation, $\frac{d\mathbf{u}}{dt}$ is the time-derivative of the input, $Q(\Delta \mathbf{z})$ is the performance output error weighting function and S is an input weighting scalar.

Both Q and S are positive definite. The performance output error weighting function is used to penalize the overshoot more intensively than the break down in the following piecewise defined form:

$$Q(\Delta \mathbf{z}) = \begin{cases} e^{a\Delta \mathbf{z}} & \text{if } \Delta \mathbf{z} > 0, \\ 1 & \text{otherwise.} \end{cases} \quad (16)$$

The parameter a is set so that the weight at the maximal prescribed overshoot is 5.

With the above cost function and the constraint made on the input variable the problem can be solved by discrete numeric optimization. For this purpose the simplex search algorithm [5] was used. The considered input actuation time interval was 400 ms. This interval was evenly divided into 10 segments (i.e. each segment was 40 ms long), where the input voltage given to the system in the corresponding

segment could be 0 V or the supply voltage (24 V). By increasing the number of the input time interval divisions one can obtain more accurate setup of the performance output after the transient phase, but it is more demanding from numeric optimization point of view because of the more possible local minimum loci. The considered constant duration of the air consumption was 250 ms.

4.5.2. Optimization Results

Fig. 6 shows optimized model responses for two cases. The input voltage profile for the individual fixed programmes are shown in Table 2, where 0 refers to the off phase and 1 to the on phase of the input voltage. The model parameter setup used for the simulation calculations is seen in Table 3.

Table 2. Input entries of the individual fixed programmes

Programme	Input Segments									
	1	2	3	4	5	6	7	8	9	10
P1	0	0	0	0	0	0	0	0	0	0
P2	1	1	1	1	1	1	1	1	1	1
P3	0	0	0	0	0	1	1	1	1	1
P4	0	0	1	0	0	0	1	1	1	1
P5	0	0	1	0	0	1	1	1	1	1
P6	0	0	0	0	0	0	0	1	1	1
P7	0	0	0	0	0	1	1	1	1	1
P8	0	0	0	0	1	0	1	1	1	1
P9	0	0	0	0	0	0	0	0	0	1
P10	0	0	0	0	0	0	0	0	1	1
P11	0	0	0	0	0	0	1	1	1	1

In conclusion the properties of the obtained input programmes are as follows. In case of low input pressure (P3, P4 and P5) a single long off-block followed by an on-block are applied. As the input pressure increases considering the same air consumption the first on-intervention shifts to an earlier segment (e.g. P9 vs. P10). As the air consumption gets higher assuming the same input pressure level, the first on-intervention shifts to a later one (e.g. P8 vs. P11).

5. Conclusions

A single circuit electro-pneumatic protection valve was investigated in this paper from control design point of view that is intended to be used for circuit pressure limiting.

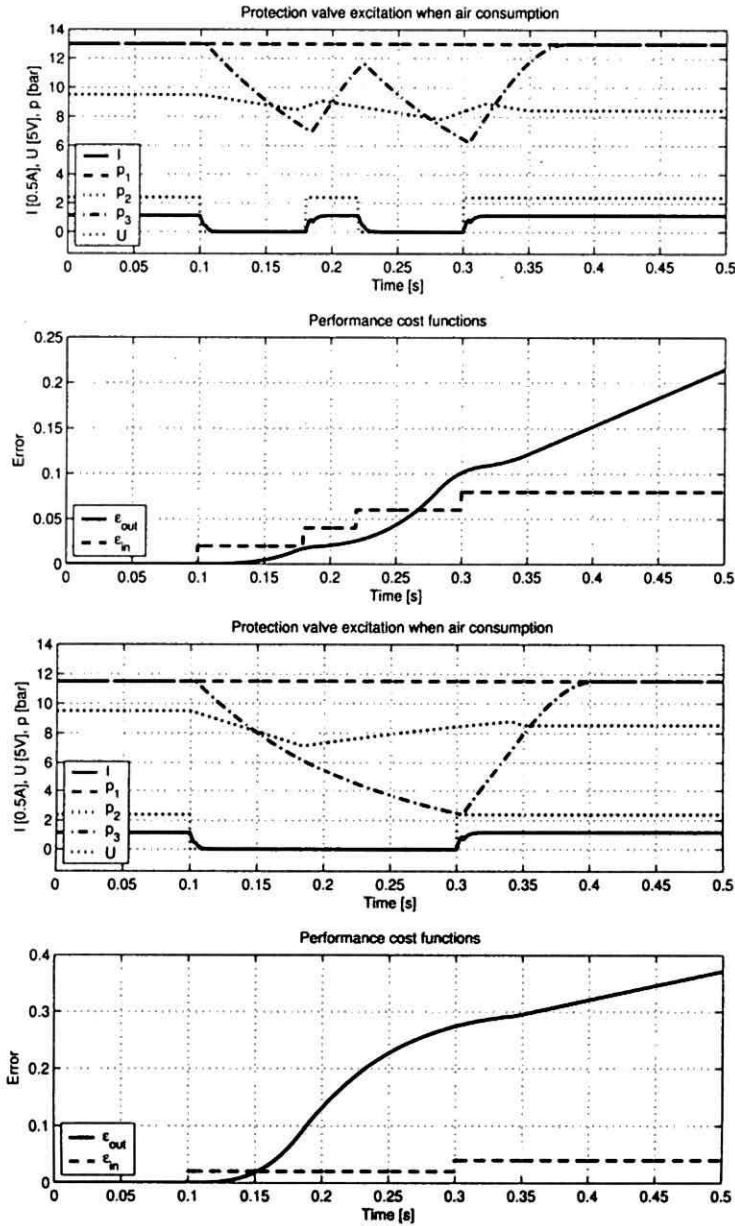


Fig. 6. Two response functions obtained by optimizations (P5 and P7 programmes)

A simplified nonlinear hybrid model containing three independent hybrid parts has first been analyzed for its dynamical properties. By analyzing the hybrid

properties it was shown that all the hybrid states are reachable in the whole operation domain of the controller. It was also shown that the model is structurally state controllable and observable, and has maximum relative degree. These properties are invariant with respect to the hybrid state changes.

Based on the control aims and input level restrictions a bang-bang control is proposed in feedforward operating mode. The applied input profiles are determined for different operation ranges by optimization, which considered output deviation and input energy terms.

Due to causality reasons a restricted part of the control problem was considered only with the assumptions of constant duration and level of external air consumption. The control included an observer for the unmeasurable key disturbance signal. The simulation results have shown that the circuit pressure limitation with the predefined overshoot tolerance is fulfilled.

Acknowledgement

This work has been supported by the Hungarian Science Fund (OTKA) through grant T042710, which is gratefully acknowledged.

References

- [1] HANGOS, K. M. – CAMERON, I. T., *Process Modelling and Model Analysis*, Academic Press, London, 2001.
- [2] ISIDORI, A., *Nonlinear Control Systems*, Springer, Berlin, 1995.
- [3] JOHANSSON, R. – RANTZER, A., *Nonlinear and Hybrid Systems in Automotive Control*, Springer, London, 2003.
- [4] KAILATH, T., *Linear Systems*, Prentice Hall, Englewood Cliffs, 1980.
- [5] NELDER, J. A. – MEAD, R., A Simplex Method for Function Minimization, *Computer Journal* 7(3) (1965), pp. 308–313.
- [6] NÉMETH, H. – AILER, P. – HANGOS, K. M., Nonlinear Modelling and Model Verification of a Single Protection Valve, *Periodica Polytechnica Ser. Transportation Eng.*, 30 No. 1–2 (2002), pp. 69–92.
- [7] NÉMETH, H. – HANGOS, K. M., Nonlinear Control of an Electro-Pneumatic Protection Valve for Circuit Pressure Limiting, Technical Report SCL-005/2003, Computer and Automation Research Institute, Budapest, Hungary, 2003, <http://daedalus.scl.sztaki.hu>.
- [8] NÉMETH, H. – HANGOS, K. M., System Identification of an Electro-Pneumatic Protection Valve, *Gép*, 56 No. 3–4 (2003), pp. 33–42, (In Hungarian).
- [9] NÉMETH, H. – PALKOVICS, L. – HANGOS, K. M., Model Simplification of a Single Protection Valve; A Systematic Approach, Technical Report SCL-004/2002, Computer and Automation Research Institute, Budapest, Hungary, 2002, <http://daedalus.scl.sztaki.hu>.
- [10] PARNICKUN, M. NGAECHAROENKUL, C., Kinetic Control of a Pneumatic System by Hybrid Fuzzy PID, *Mechatronics*, 11 No. 8 (2001), pp. 1001–1023.
- [11] SARKAR, D. – MODAK, J. M., Optimisation of Fed-Batch Bioreactors Using Genetic Algorithms: Two Control Variables, In: *European Symposium on Computer Aided Process Control*, 13 (2003), pp. 1127–1132.
- [12] WANG, J. – PU, J. – MOORE, P., A Practical Control Strategy for Servo-pneumatic Actuator Systems, *Control Engineering Practice*, 7 No. 12 (1999), pp. 1483–1488.

A. Appendix – Nomenclature

Variables

A	area, surface [m^2]
α	contraction coefficient [-]
c	spring coefficient [N/m]
d	diameter [m]
\mathbf{d}	disturbance vector
I	electric current [A]
k	damping coefficient [Ns/m]
κ	adiabatic exponent [-]
m	mass [kg]
σ	air flow [kg/s]
μ	permeability [Vs/Am]
N	solenoid turns [-]
p	absolute pressure [Pa]
R	resistance [electric- Ω ; magnetic-A/Vs]
R	specific gas constant [J/kgK]
t	time [s]
T	absolute temperature [K]
u	cross section factor [-]
\mathbf{u}	input vector
U	voltage [V]
v	speed [m/s]
V	volume [m^3]
x	stroke [m]
\mathbf{x}	state vector
\mathbf{y}	measured output vector
\mathbf{z}	performance output vector

Indices

0	refers to initial state or vacuum
1	refers to input chamber
2	refers to output chamber
3	refers to control chamber
∞	refers to limit in infinity
PV	refers to protection valve
MV	refers to magnet valve
S	refers to brake system
env	refers to environment
in	refers to inlet
exh	refers to exhaust
max	refers to maximum
MB	refers to magnet valve body – armature
ML	refers to magnetic loop of constant members

B. Appendix – Model Parameters

Table 3. Model parameters

Parameter name	Symbol	Unit	Value
Adiabatic exponent	κ	-	1.4
Permeability of vacuum	μ_0	Vs/Am	$4\pi \cdot 10^7$
Specific gas constant	R	J/kgK	287.14
Stiffness of MV spring	c_{MV}	N/m	1500
Stiffness of PV spring	c_{PV}	N/m	10000
Diameter of PV piston	d_1	m	0.018
Valve seat diameter of PV	d_2	m	0.01
MV armature diameter	d_{MB}	m	0.01
MV inlet port diameter	d_{MVin}	m	0.0007
MV exhaust port diameter	d_{MVexh}	m	0.0006
Mass of MV armature	m_{MV}	kg	0.002
Mass of PV piston	m_{PV}	kg	0.02
Number of solenoid turns	N	-	1500
Electric resistance of MV	R	Ω	42.16
MV cross section factor	u_{MV}	-	$2 \cdot 10^4$
PV cross section factor	u_{PV}	-	10^5
Output chamber volume	V_2	m^3	0.001
Control chamber volume	V_3	m^3	$5 \cdot 10^{-6}$
Spring preset stroke of MV	x_{MV0}	m	0.002
Maximal MV stroke	x_{MVmax}	m	0.0005
Spring preset stroke of PV	x_{PV0}	m	0.009
Maximal PV stroke	x_{PVmax}	m	0.002
MV contraction coefficient	α_{MV}	-	0.6834
PV contraction coefficient	α_{PV}	-	0.2966
Damping coefficient of MV	k_{MV}	Ns/m	2
Damping coefficient of PV	k_{PV}	Ns/m	10
Magnetic loop resistance	R_{ML}	A/Vs	$1.843 \cdot 10^7$